International Journal of Water Resources and Environmental Engineering Vol. 4(11), pp. 339-351, November 2012
Available online at http://www.academicjournals.org/IJWREE
DOI: 10.5897/IJWREE12.002
ISSN 1991-637X ©2012 Academic Journals

Full Length Research Paper

Messinian salinity crisis impact on the groundwater quality in Kert aquifer NE Morocco: Hydrochemical and statistical approaches

Elgettafi Mohammed[1,2]*, Elmandour Abdennabi[2], Himi Mahjoub[1], Casas Albert[1] and Elhaouadi Boubker[3]

[1]Water Institute. Departamento de Geoquímica, Petrología y Prospección Geológica. Facultad de Geología. Universidad de Barcelona. Martí i Franquès, s/n, 08028 Barcelona, Spain.
[2]GEOHYD Laboratory, Université Cady Ayyad, Faculté des sciences Semlalia, Marrakech, Morocco.
[3]Laboratory of Hydraulic Agency of Moulouya Basin, Oujda, Morocco.

Accepted 28 June, 2012

Groundwater's studies at middle Kert aquifer in northeast of Morocco are very important due to the semi-arid character and its geological history. The region is recognized by messinian salinity crisis already 5.6 Ma. Water chemistry is mainly dominated by dissolution of evaporate rocks (Halite and Gypsum) related to outcropping and basement limits developed in Messinian age. Freshwater with total dissolved solids 740 mg/l (average value) in Tafersite district is chemically distinct from saline water with total dissolved solids of 9803 mg/l in the south zone. In wadis, water is $S0_4$-Cl-Ca type; they are influenced by the surrounding highlands located at the south of the plain. The investigation reveals that weathering of evaporated rocks is the processes responsible for high Na^+, Ca^{2+}, Mg^{2+}, Cl^- and SO_4^{2-} concentrations. Also, hydro chemical data displays that freshwater observed in the northwest part reflect the influence of freshwaters coming from metamorphic massive of Temsamane. The factorial analysis reveal three sources of salinization, the principal one is described above, whilst the dissolution of carbonates and human influence represented by NO_3^-, played only a secondary role.

Key words: Salinization, groundwater, Messinian crisis, hydrochemistry, statistical, Kert aquifer, NE Morocco.

INTRODUCTION

The messinian salinity crisis was a geological event during which Mediterranean Sea went into complete desiccation throughout the Messinian age from 5.6 to 5.33 Ma (Roveri et al., 2008). The principal cause of this event was the isolation of Mediterranean basin from the Atlantics Ocean for a longer period after the closure of Atlantic gateways. Several messinian salt deposits are outcropping in many basins like Sorbas and Nijar in south Spain (Braga et al., 2006; Soria et al., 2008) and in northeastern Moroccan Neogene basins. A major question remains concerning the impact of messinian salinity crisis on the groundwater quality. Many works in northeastern of Morocco showed that salinity increases in the majority of aquifers. In shallow coastal aquifer of Saidia, the water is brakish (Melloul et al., 2007). In Triffa plain the electrical conductivity varies between 600 and 11 120 µs/cm, and the chemical facies is Cl-Na (Elmandour et al., 2008). In Bou Arg unconfined aquifer, in northeastern Mediterranean coast, the higher values of hydraulic conductivity facilitates seawater intrusion (El yaouti et al., 2009). The causes of this salinization are almost similar in all of the aquifers and linked to geological, geochemical contexts of the plains, dissolution of gypsum

*Corresponding author. E-mail: melgettafi@ub.edu. Tel: +34934035737. Fax: +34934021340.

indicated by high sulfate concentrations, and other phenomena, such as oxydoreduction reaction and ionic exchange. Thus, the problems associated with natural saline groundwater, salt-water intrusion, and upcoming of saline water due to over- pumping in agricultural and industrial zones are major concerns in many regions in the global world.

Water resources available in northeast of Morocco are scarce, vulnerable to salinization and increasingly becoming major complicating factors in the socio-ecologic and ecopolitic problems of the region. The main reasons for this issue are related to their reception input of many different water sources (seawater, rivers, sebkha and anthropogenic sources) in the one hand, in the other hand the often density populated regions. Considering the quantity and quality of water needed to satisfy the socioeconomic development in the region, freshwater is the most binding constraint and present great challenge. Like in many parts of Morocco, salinization is presented generally where aquifers are located in the riffain southern corridor or in contact with Mediterranean Sea (Elgettafi et al., 2007). This problem becomes more disturbing when it is combined with arid climate and after the long dry periods. During the last decade, the deterioration of superficial water and groundwater is a problem for the local authorities and a major scientific concern. The continued stress on land and water resources has disturbed the natural balance and has accelerated the natural salinization process, particularly in arid and semi arid climatic region. To put a limit to these dramatic changes, in 1995, the Moroccan government has adopted a 10-95 law for using the water resources. Now, 10-95 law by the high council for water and climate formulates general guidelines for the national water policy and examines the national strategy for observing climate change and its impact on water resources.

Freshwater strongly affected by interaction with minerals of the geological reservoir (Manno et al., 2007; Melish et al., 2008), is primarily controlled by weathering of aluminosilicates, dissolution of carbonate and evaporate minerals and cation exchange reactions. Thus, the knowledge of groundwater chemistry is the first requirement for many practical purposes. Hydrochemistry is an essential tool for understanding the groundwater evolution (Pilla et al., 2006). It provides information on the water provenance, residence time, flow direction and relation with surface waters. The challenge is to understand the salt sources, and the mechanisms which are responsible in incrementing groundwater salinity, in order to manage and share these water resources under those specific climate change and population growths (Elgettafi et al., 2011). The aim of this study was to investigate the geochemical characteristics of water in order to identify the main hydro geochemical process controlling the chemical composition based on major ion chemistry and statistical method.

Study area

Geological setting

The Kert basin, which covers a total area of about 250 km^2, is located in the northeastern part of Morocco and extends between latitudes 34°55' and 35°54'N, and longitudes 3°19' and 3°34'W (Figure 1). The Kert River is the important river in the Kert basin, which is mostly characterized by a seasonal flow regime. This stream with a total long rounded 90 km and a catchments area rounded 2710 Km^2 (Zielhofer et al., 2008). The kert depression received during the Miocene to Villafranchian a very mixed and varied thick marine and continental sedimentation. It is limited to the east by the western Gareb range. The massive metamorphic of Temsamane, which limits the plain in the north and northwest was affected by a compressive tectonic event generating a N120ºE fracture cleavage associated with green shale (Frizon de lamotte, 1985). In the south part we found intra rifain nappes and marls of Miocene. The Jurassic and Cretaceous deposits mostly constitute of carbonates rocks; limit the plain in the southern part (Figure 1). Several studies have been done to date the opening of Kert basin. During early-middle Tortonian, a series of conjugate strike-slipe faults (N70ºE to N90ºE) occurs east of Nekor fault, related to the formation of Kert basin (Ait Brahim et al., 2002). While, Azdimousa et al. (2007) suggest that the younger normal fault system records N-S extension controlling the formation of the Kert Basin dates the Messinian-Pliocene age. In the Messinian, Kert basin deepened with the Messinian Sea level rise (Haq et al., 1987). It is known that in the occidental Mediterranean Neogene basin the sedimentological history is marked by evaporite series related to messinian salinity crisis caused by closing of Gibraltar strait. Whereof, Hervouet (1985) defined a complex tectono-sedimentary (Gareb-Kebdana chaotic unit) extending from Kebdana in the east towards the Midar city in the west, often composed by a gypseous marl. In the west of plain, the scrapes were principally a fragment of gravity-driven napes of internal and external rifain domain slided westward along the foreland (Hervouet, 1985). The plain contains a transgressed post nappe deposits (Azdimousa, 1999). The micro paleontological dating of the sedimentary filling the Kert basin indicates late Miocene and Pliocene ages (Feinberg, 1986).

Hydrogeological setting

The hydrogeology character of the study area were described by Carlier (1973), based on data obtained from pumping tests and electrical geophysics. There is an

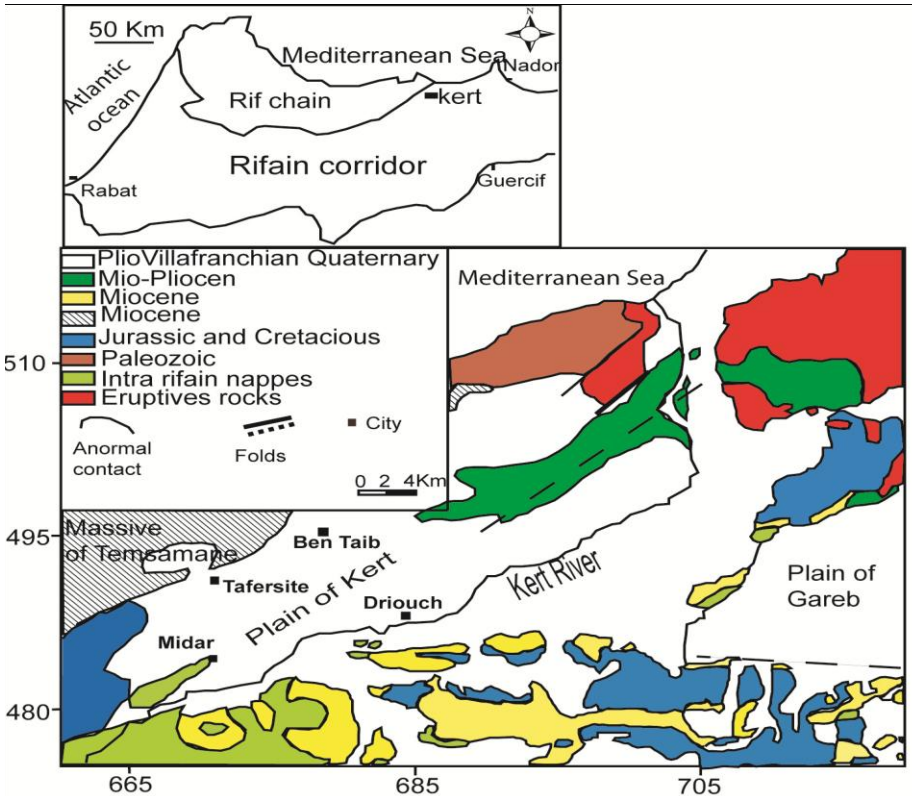

Figure 1. Geological map of Middle Kert plain (Carlier, 1973).

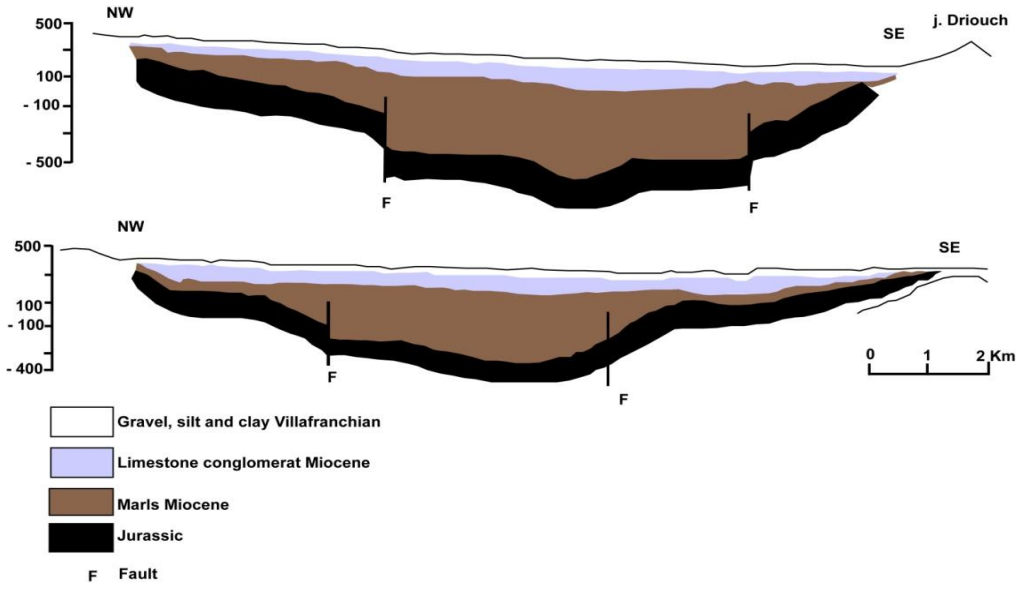

Figure 2. Hydrogeological cross section in the Kert plain (Carlier, 1973).

unconfined aquifer, which extends under the Kert plain and flows on the Miocene blue marls (substratum of aquifer). The strata of various hydrogeological formations can be identified as follows (Figure 2). The substratum of the aquifer is represented by the Miocene transgressed marls, which is overlaid by a contemporary deposit made

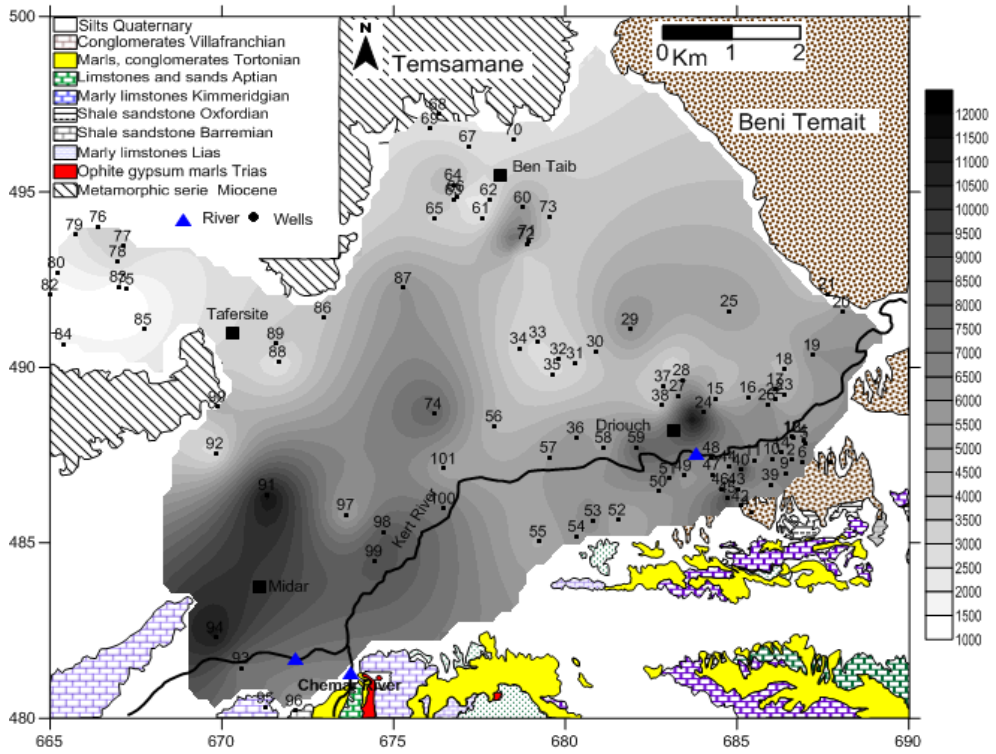

Figure 3. Electrical conductivity map of groundwater in Kert aquifer.

up of limestone and conglomerate. We assume that the Miocene formation contains the gypsum as well as the one outcrop in the region. The series end with gravel, silt and clay Villafranchian age. Two vertical faults have controlled the Kert basin during the Miocene. These faults have collapsed the center of the plain and have raised the borders north and south. Consequently, the aquifer might be hydraulically connected through those faults with the underlying Jurassic unit. Two exploratory boreholes were drilled in this latter unit in order to find an aquifer in the deep resisting formation determined by geophysics (Zeryouhi, 1971). The first borehole number is 1635/6 with the depth of 801m (X = 685.18 Y = 486.85 Lambert coordinates) and the second borehole number is 1636/6, 684 m in depth (X = 679.14 Y = 484.05 Lambert coordinates). Both of them had not given the expected result.

Thirty-two Pumping tests were performed on the plain. Permeability and transmissivity computed using classical Theis-Jacob method amount from 0, 4.10^{-5} to 18.10^{-5} m/s and from 0, 1.10^{-3} to 34.10^{-3} m^2/s, respectively. Storage coefficient estimated from these tests is 0.3 to 3.5%. The piezometric head contour map realized in 2008 (Elgettafi, 2011) shows that in northern part water flow from Northwest to Southeast. The second water flow as the major direction is from West to East in centre plain. Temsamane massif metamorphic located on the northwestern side is considered as a recharge zone for the studied groundwater. The discharge fields are situated in the extreme East. Kert River is characterized by a seasonal flow regime and it is in connection with aquifer.

MATERIALS AND METHODS

Water sampling

A total of 94 wells and 3 surfaces waters samples (Kert in Midar, Kert in Driouch and Chemar) were collected during two field trips in July and in December, 2008. Locations of water sampling points are showing in Figure 3. All the data in the study area are listed in Table 1. The pH, Tp, and specific electrical conductivity (EC) measurements were maked *in situ*. The electrical conductivity was measured simultaneous with temperature by a VWR EC300 instrument, previously calibrated by the conductivity solution HI 70031 (HANNA). pH measurements were carried out using a glass electrode connected to a VWR pH100-meter, after calibration with pH 4.01 and 7.00 buffer solutions. Each sample was stored in new polypropylene bottle, pre-washed with HNO_3 and rinsed with deionized water. The bottles were capped without leaving any head space and stored in a refrigerated container for transport to the laboratory and kept cool until analysis. All of the water samples, were analyzed for major cation (Na^+, K^+, Ca^{2+}, Mg^{2+}) major anions (Cl^-, SO_4^{2-}, HCO_3^-, NO_3^-), and total dissolved solids (TDS), in Hydraulic Laboratory of Moulouya Agency, Oujda, using standard analytical procedures. Ca^{2+}, Mg^{2+}, Cl^- and HCO_3^- were determined by titrimetric methods. The concentration of Na^+, k^+, SO_4^{2-} and NO_3^-

Table 1. Hydrochemical analyses of groundwater in Kert aquifer (electrical conductivity, total dissolved solids,temperature, sodium, potassium, calcium, magnesium, chloride, bicarbonates, sulphate and nitrates, KD, Kert in Driouch; KM, Kert in Midar; CH, Chemar).

ID wells	EC	TDS	Tp	Ph	Na	K	Ca	Mg	Cl	HCO_3	SO_4	NO_3
1	6470	4966	24	7.41	1240	7	212	250	1659	298	1258	17
2	6310	4944	21	7.22	1120	5	240	315	1399	292	1460	34
4	5860	4393	22	7.32	720	5	200	243	1249	305	1317	32
5	6990	5093	23	7.07	620	5	440	157	1499	280	816	14
6	6780	5324	22	7.05	560	5	444	174	1549	274	781	22
9	7190	5855	22	7.02	600	6	400	187	1374	280	1181	18
10	7260	5322	26	7.2	640	6	420	218	1629	286	1338	38
11	5810	4317	20	7.09	660	5	408	153	1099	305	1132	35
12	5940	4413	20	7.16	520	5	424	155	1349	317	1111	39
13	6313	4600	19	7.4	550	5	408	170	1409	347	1030	35
14	6050	4112	20	7.21	560	5	320	182	1449	280	1022	26
15	4460	2991	22	6.95	630	8	268	68	1124	549	663	31
16	5120	3222	21	6.98	780	7	280	72	1084	610	740	35
17	5240	3602	22	6.77	720	8	192	162	1189	610	920	28
18	4210	2944	23	6.99	600	6	180	133	974	610	765	23
19	6060	3998	21	6.96	830	7	248	148	1774	427	736	18
20	5640	4369	23	7.06	920	8	172	223	1584	366	618	23
21	3980	2853	22	7.36	680	6	116	155	1074	366	438	20
22	4540	2986	22	6.75	960	9	168	140	924	854	850	15
23	4780	3196	21	6.89	1000	9	148	165	1049	841	830	16
24	12300	9803	21	6.96	2500	6	300	464	3398	317	1683	145
25	5570	4641	21	7.19	840	5	521	29	1599	305	430	15
26	6720	3814	21	6.8	800	9	240	140	1399	628	813	11
27	6050	4249	22	7.25	1120	6	352	65	1374	408	1166	31
28	5860	3976	23	7.02	1200	5	360	77	1369	390	1054	20
29	6360	5133	22	7.17	1160	5	376	140	2099	305	644	18
30	3970	2592	26	6.8	680	5	232	102	674	744	689	19
31	3070	2053	23	7.21	460	4	184	70	704	335	361	10
32	3040	2143	25	7.16	480	4	220	60	669	317	550	18
33	2970	1945	24	7.22	420	4	168	85	684	292	320	9
34	3050	2287	26	7.21	500	4	240	80	664	292	520	22
35	2840	1800	23	7.24	440	5	192	89	554	353	507	18
36	5920	4621	22	7.08	1000	5	432	211	1159	335	1444	28
37	4280	2739	22	7.1	680	13	240	70	1009	366	532	11
38	3480	2244	22	7.06	700	5	240	72	689	414	656	27
39	6010	4227	23	7.32	1280	7	320	228	1874	286	997	2
40	9800	7871	22	7.14	2100	8	581	352	2949	305	2029	9
41	6821	3104	24	7.21	1040	9	228	116	1199	402	1066	6
42	6320	2233	23	7.45	720	10	180	189	1289	347	1108	8
43	5820	5780	22	7.27	1900	7	432	296	2664	268	1519	7
44	6010	2635	22	7.1	920	6	368	165	1024	335	1472	6
45	9800	5614	23	7.13	2000	8	521	291	2499	305	2013	8
46	6820	2882	22	7.11	1040	7	320	216	1399	323	1562	7
47	6320	2806	21	7	1000	6	360	170	1099	366	1558	6
48	5820	2904	22	7.12	760	4	372	162	1024	335	1489	6
49	5500	2901	23	7.22	600	5	236	123	774	317	1148	13
50	5800	3750	22	7.31	820	8	240	182	1124	427	1305	7
51	6990	4783	21	6.85	840	6	420	194	1454	317	1313	36

Table 1. Contd.

52	4910	3251	21	7.56	750	5	216	167	1334	292	1289	7
53	6400	4326	22	6.85	880	6	300	194	1324	396	1307	8
54	5860	3864	21	7.27	800	5	276	160	1349	311	1250	7
55	4830	3381	21	7.16	730	5	240	145	819	323	1419	6
56	4390	2319	22	6.94	700	8	184	77	749	854	593	8
57	5540	3618	22	7.1	620	5	360	145	914	317	1564	15
58	5310	3449	23	7.15	630	5	318	145	874	323	1444	14
59	8360	5828	22.5	7.17	790	6	525	252	1774	280	1736	41
60	6040	4079	23.5	7.2	480	6	448	128	1849	183	416	43
61	2410	1306	22	7.56	290	3	116	68	509	256	324	16
62	2460	1286	23	7.52	290	3	136	61	514	250	326	52
63	3710	2254	22	7.16	400	4	224	92	864	286	414	12
64	4860	2364	21	7.16	470	5	381	182	1359	329	883	9
65	3320	2231	22	7.34	340	3	212	124	769	347	660	0
66	2000	1101	22	7.66	270	6	128	58	394	323	393	103
67	2840	1683	23	7.32	310	3	212	70	649	341	405	81
68	2160	1122	23	7.52	260	2	160	63	469	366	442	19
69	2700	1577	22	7.31	300	4	168	83	569	366	550	35
70	2570	1548	22	7.58	300	5	140	92	659	305	432	36
71	8550	5572	22.5	6.85	850	8	533	201	2124	762	1168	38
72	3450	2159	21.5	7.36	400	5	220	78	934	317	420	36
73	3620	2355	22	7.7	370	5	240	102	969	274	381	36
74	8240	3559	22	6.74	610	9	357	63	424	719	1187	6
75	1120	377	21	7.44	42	0.34	88	27	109	274	91	10
76	3580	1502	22	7.24	150	1	272	53	374	329	412	21
77	2850	1065	23	7.18	150	0.67	160	36	284	329	269	6
78	3250	1332	23	7.1	130	0.67	212	53	324	335	387	0
79	2400	861	23	7.26	80	0.33	136	29	239	335	148	5
80	1750	615	23	7.3	70	0	100	29	199	335	69	9
81	1190	389	22	7.36	140	0.33	92	34	174	305	126	4
82	1080	357	21	7.5	160	0.67	80	27	124	280	142	4
83	1120	349	22	7.52	180	0	80	22	134	280	132	8
84	1700	750	22	7.33	40	0.67	160	39	174	262	306	0.42
85	1490	546	21	7.37	80	0.67	116	46	124	329	232	0.33
86	3860	1682	23	7.19	360	1.67	220	75	529	311	626	1
87	6130	2500	23	7.57	470	6	180	104	999	183	695	2
88	2180	821	23	7.4	210	2	152	44	249	274	412	0
89	3720	1551	22	7.2	300	5	232	49	514	366	526	0
90	4800	1869	24	6.88	440	3	232	87	574	713	687	0
91	11800	4381	22	6.47	990	18	244	151	1499	1329	822	0
92	2520	724	23	7.24	260	2	160	97	189	579	856	0
93	7190	3726	23	7.11	570	5	348	243	799	323	2013	1
94	11300	5926	22	6.23	660	5	553	211	1174	1311	306	1
95	7130	3074	23	6.95	610	5	280	170	1079	488	1295	3
96	5440	2442	22	6.99	440	2	268	116	634	366	844	0
97	5180	2323	22	7.04	500	4	160	194	564	457	1542	0
98	8570	4008	21	6.73	670	4	360	255	1109	579	1840	1
99	8780	4286	22	6.85	510	4	472	223	1049	549	1876	0.2
100	7160	3409	22	7	520	3	400	145	764	427	1815	0.4
101	5080	2416	21	7.13	390	3	296	121	624	445	1256	1

Table 1. Contd.

Wadis										
KD	4850	3928	560	5	737	39	780	165	1642	27
KM	4070	3877	460	7	705	29	840	165	1673	0
CH	5130	4212	740	7	753	97	900	165	1550	0

was measured by atomic absorption spectrophotometry. The values of Charge Balance Errors are less than or equal 5%, which is an acceptable error for the purpose of this study:

$$CBE = \frac{\sum Cations - \sum Anions}{\sum Cations + \sum Anions}$$

The theoretical partial pressure of CO_2 in water (P_{CO2}) was calculated with thermodynamic model PHREEQC (Parkhurst and Appelo, 1999).

Statistical method

Generally, hydrological and geochemical processes are difficult to understand on account of their complexity. However, based on hydro chemical composition, statistical method can show the correlations between them. A correlation analysis was applied to describe the degree of relation between two or more hydro chemical parameters. A high correlation coefficient near 1 or -1 means a good relationship between variables, and a correlation coefficient around 0 means no relationship.

The correlation coefficient is:

$$r_p = \frac{\sum_{i=1}^{N}(x_i - \bar{x}) \cdot (y_i - \bar{y})}{\sqrt{\sum_{i=1}^{N}(x_i - \bar{x})^2} \cdot \sqrt{\sum_{i=1}^{N}(y_i - \bar{y})^2}}$$

This expression is simply the sum (over all samples) of the product of the deviations of the x_i measurements and the y_i measurements on each sample from the mean values $\bar{x}$ and $\bar{y}$ respectively for the complete set of samples.

Principal component analysis (PCA) and factor analysis (FA) were applied to explain relationships between variables and thus, infer the processes that control water chemistry (Helina et al., 2000). The main purpose of FA is to reduce the contribution of less significant variables to simplify even more of the data structure coming from PCA. This method starts by coding all variables to have zero means and unit variances, and find the eigenvalues and corresponding eigenvectors. Then, the data were transformed to factors. The factor extraction was done with a minimum acceptable eigenvalue as 1 (Mahlknecht, 2004). Orthogonal rotation of these initial factors to terminal factor solution was done with Kaiser's varimax scheme (Kaiser, 1958). The operation finish by factors scores coefficients, which are derived from the matrix loading.

RESULTS AND DISCUSSION

Water hydrochemical

Analyses of chemical results show a large variation in chemical compositions and also indicate low salinity of some groundwater samples (Tafersite region). TDS values are 349 to 9803 mg/l, knowing that the values greater than 1000 were considered indicative of salinity (Petalas and Diamantis, 1999; Jalali, 2006) nevertheless, in arid zone where the water is scarce; water bad quality is currently used. SEC values are in the range of 1080 to 12300 µs/cm. Generally, the ionic content of groundwater of the study area is high, the dominant cations are Na^+ and Ca^{2+} (max value are 2500 and 581, respectively) and the dominants anions are Cl^- and SO_4^- (max value are 3398 and 2029, respectively). HCO_3^- ranges from 183 to 1329 mg/l; the high concentration corresponds to the low values of pH. Water CO_2 partial pressures range between $10^{-2.3}$ and $10^{-0.1}$ atm, and all of the samples had P_{CO2} over values significantly above of the atmosphere because of the possible contribution of biologic respiration. As to NO_3^- the over concentration is seen in some wells, it means that the contamination is local, and is likely to be derived from the use of traditional fertilizers (animal waste). A significant feature of these waters is their weak acidic character, with pH values in the range 6.23 to 7.66, and temperature ranges from 19ºC to 26ºC, reflecting that water circulates in the same depth. The geochemical modeling program PHREEQC (Parkhurst and Appelo, 1999) was used to calculate aqueous speciation and the thermodynamic equilibrium conditions of waters with respect to the main mineral phases present in the aquifer. Saturation indices, defined as SI=log (IAP/Kt), IAP being the ion activity product of the mineral-water reaction and Kt the thermodynamic equilibrium constant at the measured temperature, were calculated by ion activities. Thus, SI=0 indicates a thermodynamic equilibrium state, and values >0 and <0 denote super saturation and under saturation, respectively. All the groundwater samples are supersaturated with respect to calcite and dolomite (from 0.04 to 0.83 and from 0.3 to 1.61 respectively), and under saturated with respect to gypsum and halite (from -1.52 to -0.32 and from -6.8 to -3.8, respectively).

As for the wadis's samples they all show high salinity. They are 5130 µs/cm in Chemar and 4850 µs/cm in Kert near Driouch city. The oversaturation in Kert wadi (4850 µs/cm) is detected after its connection with Chemar Wadi. The dominant cations are Na^+ and Ca^{2+} (max value are 740 and 817 mg/l, respectively), and dominant anions are SO_4^{2-} and Cl^- (max values are 1720 and 900 mg/l, respectively) (Table 1).

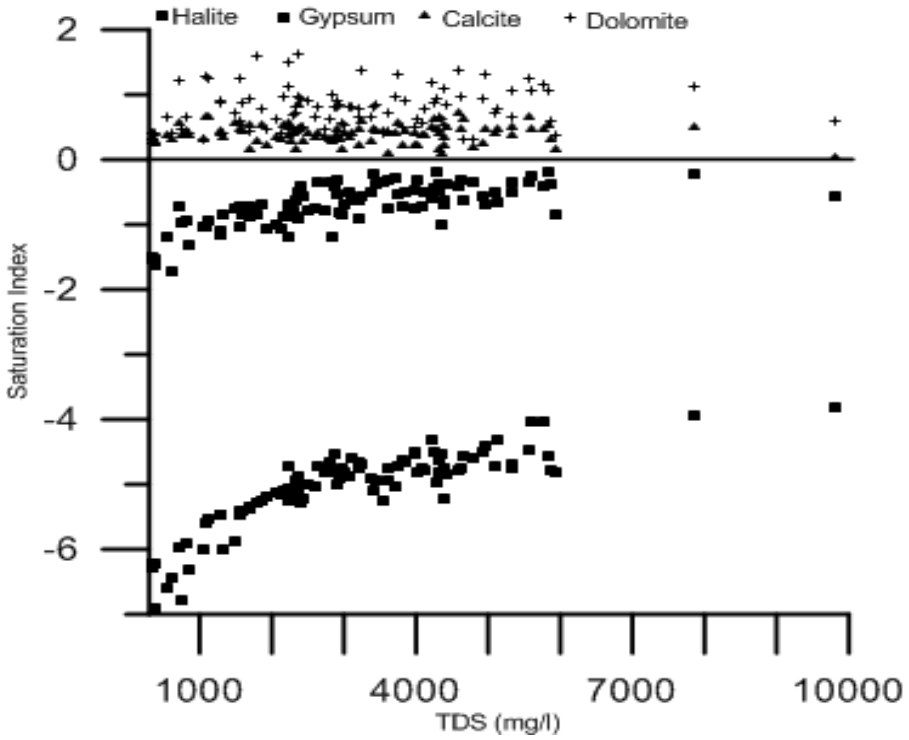

Figure 4. Relationships between TDS and SI of Halite, Gypsum, Calcite and Dolomite.

Geochemical process

The spatial distribution of electrical conductivity indicates some contrast (Figure 3). There is a pronounced increase in electrical conductivity from the northwest margin to the centre of the field. Only one zone that consists of freshwater is distinguished which located in Tafersite in the northwest part of the study area. TDS is about 740 mg/l and EC= 1957 µs/cm, and abundance orders mE/l Ca>Na>Mg and HCO_3>Cl>SO_4. The water type is HCO_3-Ca. The low degree of mineralisation of these waters which are in contact with metamorphic massive of Temsamane suggest the laterally alimentation by fresh waters. Salinity values increase from North to South, corresponding to the main groundwater flow direction and exceed 11 000 µs/cm in Midar and Driouch (Figure 3). This salinity increase could be explained by: probably a longer contact-time with rocks during water circulation and/or depend on the distance from a source of freshwater. The second zone consists of the remaining samples that we find towards the south and presents a most important percentage. It is different from other samples in terms of its high salinity (average TDS= 3667, EC=5931). Na>Ca/Mg and Cl>SO_4>HCO_3 are dominant cation and anion element respectively. The significant character of these waters is that they are located in the zone where the upper Miocene marls both outcrop and are at 4 m of depth. Secondly the zone is crossed by kert wadi. It appears that groundwater quality is represented by a wide range of concentrations mainly dominated by evaporite rock dissolution.

This kind of waters is frequently observed in Neogene basin in northeastern of Morocco. In order to identify the salinization sources for middle Kert aquifer and to delineate the areas of influence, the hydrochemistry was analyzed graphically by means x-y plots and equilibrium state of the water with respect to a mineral phase which was determined by calculating a saturation index (SI) using analytical data.

Figure 4 shows the plots of SI against TDS for all the investigated water. It can be seen that all the groundwater samples are supersaturated with respect to calcite and dolomite. No clear tendency between carbonates Si and TDS evolution is found in all groundwater samples. That suggests the sensitivity of carbonates minerals to precipitation. Also, all the groundwater samples are under saturated with respect to halite and gypsum suggesting the dissolution of evaporates minerals. Saturation with respect to those latter is approached with increasing TDS content, although no samples reach saturation especially halite SI. This means that these elements are not limited by mineral equilibrium and variable degrees of continuous dissolution of halite and gypsum is occurred.

The same behavior is known in Bou Areg aquifer NE Morocco. Evaporates mineral phases are minor or absent in the host rock aquifer as suggested by El yaouti et al. (2009) is not supported by this study. The dissolution of

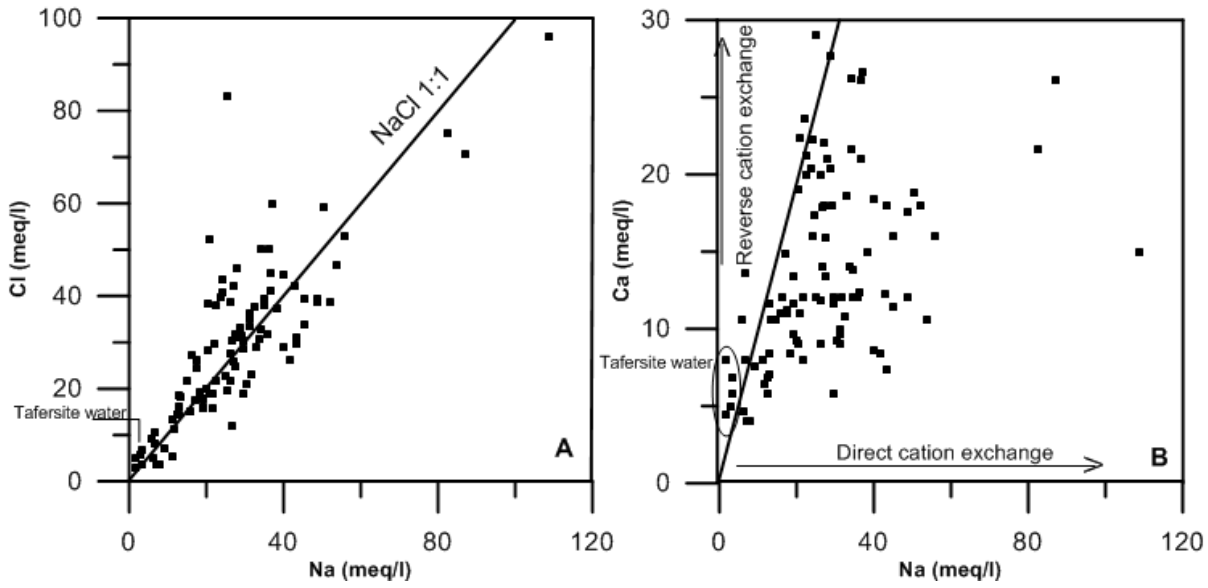

Figure 5. Relationships Na vs Cl (A) and Na vs Ca (B).

gypsum in these waters should also tend to maintain saturation or super saturation with respect to carbonate minerals. Thus, increasing of Ca^{2+} and Ca/Mg ration causing by gypsum dissolution generates systematically the phenomenon of dedolomitisation which explains the over-saturation of calcite and dolomite.

The Na-Cl scatter gram shows that generally, Na^{2+} increases linearly with Cl^- along the NaCl 1:1 line of halite minerals (Figure 5A); suggesting that the processes controlling the Cl^- ion concentration are also affecting Na^{2+}. That may be a result of weathering rock rich in NaCl (Halit), which is highly soluble and easily dissolved. Through, chloride has a conservative behavior (Tellam and Lloyd, 1986). Some wells show an excess of Na^+ with respect of Na/Cl ratio of halite minerals. This could be due to a further water source for Na^+. Thus, Na/Cl>1 may be explained by different ways.

(i) Dissolution of evaporate Na-SO_4 minerals.
(ii) Ca-Na exchange according to the reaction:

$$(Ca,Mg)^{2+} + 2Na_{ex}^{+} = (Ca,Mg)_{ex} + 2Na^{+} \quad (1)$$

(iii) The high concentration of Na^+ is related to the important water-rock interaction.

A look at the evolution of Ca relative to Na (Figure 5B) shows a mixing trend between fresh and saline water. In Tafersite region low salinity shows an excess of Ca^{2+} with respect Na-Ca line. This behavior is due to the freshwater coming laterally from the metamorphic massive of Temsamane which border the plain in the north. It is shown by piezometric map that the aquifer is supplied by the Temsamane Mountains. This mixture diluted the groundwater within various degrees. The water has been enriched more by Ca^{2+} according to the reaction 2, than other wells (Figure 5B). We can explain that by reveres cation exchange.

$$Ca_{ex}^{2+} + 2Na^{+} = Ca^{2+} + 2Na_{ex}^{+} \quad (2)$$

Assuming that Na derives from different sources and that Cl is only from halite and also since the Na/Cl ratio it was concluded that the studied waters have been affected by cation exchange reactions causing low salinity (removed Na^+), and the excess of Na^+ in high salinity reflect extra source of Na^+.

There are several soluble sedimentary minerals that release SO_4^{2-}, Ca^{2+} and Mg^{2+} upon dissolution. The principal source of Ca^{2+} and SO_4^{2-} is the dissolution of gypsum ($CaSO_4.H_2O$) and anhydrite ($CaSO_4$). The dissolution of gypsum is fast and just a few residence time of water in gypsum land increase strongly the saturation index of gypsum. In the Ca-SO_4 diagram water in Tafersite region low mineralization depict different trends than other samples. Those samples have greater concentration of Ca^{2+} relative to SO_4^{2-} (Figure 6). It is widely accepted that SO_4^{2-} depletion has been caused by the biological reduction or precipitation of gypsum as a result of extensive evaporation. However, the condition under which precipitation of gypsum took place have not yet been clarified (Sig<0). Although, the majority of samples show a high concentration of SO_4^{2-} (Figure 6), Sulphate concentrations are variable, and increase content occurs from the recharge area (Tafersite) in the northern part towards the south. This increase may be due to the dissolution of gypsum and/or oxidation of

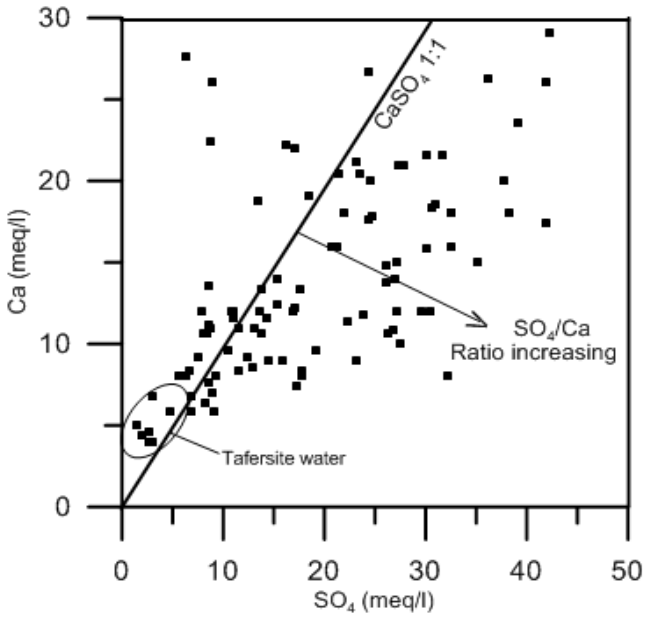

Figure 6. Relationships between SO_4 and Ca.

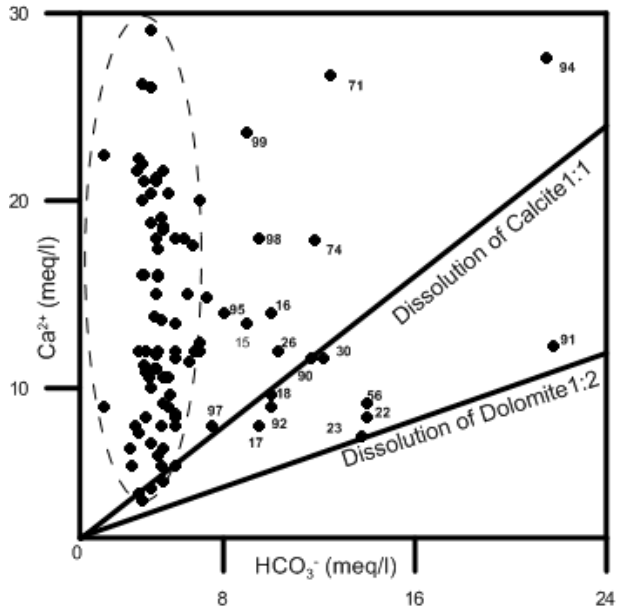

Figure 7. Relationships between HCO^-_3 and Ca^{2+}.

sulfide minerals. Also, the Kert wadi which crossed the plain in the south and hydraulically connects with groundwater is an additional source of SO_4^{2-}. The dissolution of gypsum is also accompanied by cation exchange reactions. The most important exchange reactions are the water softening reactions in Tafersite region, where Ca^{2+} and Mg^{2+} in the water exchange with sorbed Na^+ as ground water moves through clayey material. A deficit of Ca^{2+} showing in Figure 6 could be linked to cation exchange and carbonate precipitation, the both factors are known that remove the Ca^{2+} from groundwater and decrease its concentration. Their content of SO_4^{2-} and Ca^{2+} seems to be influenced by waters circulating within Miocene formation. Generally, gypsum deposits typically contain some magnesium; the dissolution of gypsum will also result in an increase in concentration of Mg^{2+} in water. The removal of Ca^{2+} and Mg^{2+}, through the dissolution of evaporate minerals, may cause a disturbance in carbonate chemical equilibrium. This is confirmed by the water oversaturation index with respect to calcium and dolomite. Besides local geology (Miocene substratum) these waters are also influenced by the lithology of the catchment area. On regional scale, the surface geology in south region is dominated by gypsum marls Messinian age, which is crossed by Kert Wadi.

The total dissolved inorganic carbon (TDIC) is equivalent to the groundwater HCO_3^- content for the observed pH range. The solubility of calcite and dolomite is largely controlled by CO_2 fugacity and pH, according to following reactions:

$$CaCO_{3(s)} + H_2CO_3 = Ca^{2+} + 2HCO_3^- \quad (3)$$

$$CaMg(CO_3)_2 + 2H_2CO_3 = Ca^{2+} + Mg^{2+} + 4HCO^-_3 \quad (4)$$

As shown previously, increasing the P_{CO2} from $10^{-2.3}$ to $8.10^{-0.1}$ atm increases the total of amount of HCO_3^- in solution from 250 to 1329 mg/l and lowers the pH from 7.66 to 6.23. So, these data are consistent with a reaction scheme in which meteoric waters flowing through the soil zone gain high CO_2 pressure and then are driven towards saturation by reaction with the carbonate minerals of the soil and host rocks. Figure 7 shows a series of samples witch show an increase in calcium content independently of bicarbonate concentration, this reflect the dominance of gypsum dissolution to increase Ca^{2+} concentration and tends to exclude its relation with weathering of carbonates.

Correlation matrix

The Pearson's correlation matrix to find the relationships between two or more variables was carried out using Stat graphics plus 5.1software as shown in Table 2. Samples showing $r > 0.6$ are considered to be strongly correlated, whereas $r < 0.6$ shows poor correlation. EC shows a good correlation with Cl^-, SO_4^{2-}, Na^+, Mg^{2+} and Ca^{2+} suggest that these elements are the principal source of salinization. The same for, Cl^-, Na^+, Mg^{2+}, Ca^{2+} and SO_4^{2-} have a good correlation between them. These data suggest that water from different samples has the same geochemical properties. Also, the good correlation of these aqueous species with Cl^- suggests that all of these

Table 2. Descriptive statistics of hydro chemical data (electrical conductivity, total dissolved solids, temperature, sodium, potassium, calcium, magnesium, chloride, bicarbonates, sulphate nitrates and pressure of CO_2).

Factor	EC	Ca	Mg	Na	K	Cl	SO_4	HCO_3	NO_3	P_{CO2}	pH
EC	1										
Ca	0.73	1									
Mg	0.76	0.53	1								
Na	0.71	0.52	0.77	1							
K	0.60	0.29	0.39	0.55	1						
Cl	0.77	0.68	0.80	0.87	0.53	1					
SO_4	0.70	0.59	0.78	0.66	0.37	0.58	1				
HCO_3	0.34	0.03	0.02	0.09	0.46	-0.01	-0.15	1			
NO_3	0.10	0.06	0.23	0.22	0.14	0.31	0.007	-0.15	1		
P_{CO2}	0.43	0.21	0.10	0.08	0.32	0.06	-0.004	0.84	-0.14	1	
pH	-0.6	-0.4	-0.25	-0.74	-0.41	-0.25	-0.28	-0.74	0.14	-0.68	1

Table 3. Loading of the components obtained from principal component analysis, with three factors, Eigenvalue derived by factor analysis, and cumulative % explained by factors.

Factor	1	2	3
Cl	0.85	-	-
SO_4	0.88	-	-
HCO_3	-	0.88	-
NO_3	-	-	0.88
Ca	0.77	-	-
Mg	0.88	-	-
Na	0.83	-	-
pH	-	-0.82	-
P_{CO2}	-	0.91	-
Eigen value	4.816	2.281	0.971
% variance	48.16	22.81	9.71
Cumulative %	48.16	70.97	80.68

species have behaved in a predominantly conservative manner with little water-reservoir rock interaction once the waters entered in the aquifer.

Factor analysis

The Varimax rotation Factor Analysis (FA) was used as an alternative tool for corroboration of the concept obtained from hydrochemistry analysis. The Stat graphics plus 5.1 were used for extracting factors through the principal extraction method. The calculated factor loading, together with communalities and percentages of variance explained each factor, are listed in Table 3 .The three retained factors explain about 80.65% of total variance of the data set (Table 3).

Factor 1 explains more than 48.31% of the variance. This factor is interpreted as related mainly to salinization of groundwater due to dissolution of evaporitic rocks. The main contributors are Cl^-, Na^+, SO_4^{2-}, Ca^{2+} and Mg^{2+}, correlate positively with EC. Association between Ca, Mg, Na, Cl and SO_4 suggest dissolution of gypsum and halite. This is also supported by geological investigations. The occurrence of process of this factor is especially in aquifer basement and Miocene marly-gypsum outcrops in the southern of plain. The component of the salinization factor is similar to dissolution evaporate process in NE of Morocco (Elmandour et al., 2008; El yaouti et al., 2009), and SE Spain (Ceron et al., 2000).

Factor 2 explaining about 22.58% of total variance, includes HCO_3^-, pH and P_{CO2}. This is strongly P_{CO2} controlled the weathering. The higher concentration in HCO_3^- may be caused by carbonate dissolution driven by the increase of PCO_2 and the decrease of pH. This process is predominant in Midar region. The weathering of carbonate rocks in this region causes the high HCO_3

concentration throughout the aquifer.

Factor 3 concerns NO_3^- (anthropogenic contamination) and contributes to total variance for about 9.75%. The high concentration is a particular case. That can be derived from sewage affluent and/or animal waste. Maximum observed NO_3^- concentration of groundwater in the study area is 145 mg/l, which is essentially higher than Moroccan standards for drinking water.

Conclusion

The present study shows that the Kert region consists of deposits from the Jurassic to Villafranchian ages. The geological and geophysics study show that the reservoir is formed by detrital deposits of average permeability and it is based on marl substratum upper Miocene (Messinian) age.

Natural recharge in the study area is extremely limited to northwest part of area study (Tafersite region), and is identified in the Temsamane metamorphic massive.

The hydro chemical data clearly indicate the contribution of local geology in salinity increasing of groundwater. The identified potential source of salinization includes dissolution of evaporate sediments which comprise the aquifer substratum. So, the abundance of SO_4^{2-}, Cl^-, Na^+, Ca^{2+}, Mg^{2+} in the groundwater is attributed to gypsum and halite dissolution. The reverse cation exchange process is important here because it has effectively increased Ca^{2+} concentration in Tafersite region at the expense of Na^+. This process is confirmed by salinity value rise and concentration variation, as a consequence of the dissolution of the aquifer materiel and cation exchange reactions between groundwater and the clay fraction .Generally, the groundwater have a similar chemical composition, they must have formed at the same time and from the same origin seawater masses. The water evolved from Messinian (upper Miocene) seawater that underwent evaporation during Mediterranean desiccation. Factor analysis is a powerful tool that gives an important clue for understanding geochemical processes that control the groundwater salinization. The statistical results show 3 factors (F1, F2 and F3), that explained 80.65% of the total variance in the groundwater quality. Factor 1 is the principal source of groundwater mineralization included Cl^-, Na^+, SO_4^{2-}, Ca^{2+} and Mg^{2+}. Factor 2 is the carbonates processes include HCO_3^-, P_{CO2} and pH. Factor 3 represented by NO_3^- explained the human impact.

REFERENCES

Ait Brahim L, Chotin P, Hinaj S, Abdelouafi A, El Adraoui A, Nakcha C, Dhont M, Charroud M, Sossey Alaoui F, Amrhar M, Bouaza A, Tabyaoui H, Chaouni A (2002). Paleostress evolution in the Moroccan African margin from Triasic to Present. Tectonophysics 357:187-205.

Azdimousa A, Jabaloy A, Asebriy L, Booth-Rea G, González-Lodeiro F, Bourgois J (2007). Lithostratigraphy and stucture of the Temsamane unit (eastern external Rif, Morocco), Revista de la Sociedad Geológica de España. 20:187-200.

Azdimousa A (1999). Géodynamique et exhumation des bordures meridionales de la mer d'alborane entre le massif de Beni Bouzera et le Cap des trois Fourches (Rif, Maroc). Apports de la méthode d'analyse par traces de fission. PhD Thesis, Univ, Mohamed I, Oujda, Maroc.

Braga JC, Martín JM, Riding R, Aguirre J, Sánchez-Almazo IM Dinares-Turell J (2006). Testing models for the Messinian salinity crisis: The Messinian record in Almería, SE Spain. Sediment. Geol. 188-189:131-154.

Carlier P (1973). Carte hydrogólogique au 1/50000 de la plaine du moyen Kert (Province de Nador, Maroc nord-oriental), Notes. Mém. Serv. Géol. Maroc, No. 250:72.

Ceron JC, Jimenez-Espinosa R, Pulido-Bosch A (2000). Numirecal analysis of hydrogeochemical of data: A case study (Alto Guadalentoan, southeast Spain). Appl. Geochem. 15:1053-1067.

Elgettafi M (2011). Caractérisation des processus de la salinisation des eaux souterraines de la plaine de Kert, Maroc, Nord Oriental: Approches hydrogéologique, géochimique et géophysique. Thése doctorale, Université de Marrakech, Maroc, p. 172.

Elgettafi M, Himi M, Casas A, Elmandour A (2011). Hydrochemistry caracterisation of groundwater salinity in Kert aquifer, NE Morocco. Geographia Technica. 2:15-22.

Elgettafi M, Elmandour A, Himi M, Casas A (2007). Origin and Distribution of Saline Groundwater at middle Kert aquifer System, (NE Morocco). Hidrogeología y Aguas Subterráneas, IGME, 23:605-614.

Elmandour A, El Yaouti F, Fakir Y, Zarhloule Y, Benavente J (2008). Evolution of groundwater salinity in the unconfined aquifer of Bou-Areg, Northeastern Mediterranian coast, Morocco. Environ. Geol. 54:491-503.

El Yaouti F, Elmandour A, Khattach D, Benavente J, Kaufmann O (2009). Salinization processes in the unconfined aquifer of Bou-Areg (NE Morocco): A geostatistical, geochemical, and tomographic study. Appl. Geochem. 24:16-31.

Feinberg H (1986). Les series tertiaires des zones externes du Rif (Maroc) (Areas tertiary series of external Rif, Morocco), Notes. Mém. Serv. Géol. Maroc, 315:192.

Frizon de Lamotte D (1985). La structure du Rif oriental (Maroc) : rôle de la tectonique longitudinale et importance des fluides (Oriental Rif structure, Morocco: Longitudinal tectonic role and fluide importance), PhD Thesis, University of Pièrre et Mairie Curie, Paris, 8-03:436.

Haq BU, Hardenbol J, Vail PR (1987). Chronology of fluctuating sea levels since the Triasic. Science 235:1159.

Helina B, Pardo R, Vega M, Barrado E, Fernandez JM, Fernandez L (2000). Temporal evolution of groundwater composition in an alluvial aquifer (Pisuerga River, Spain) by principal component analysis. Water Res. 34:807-816.

Hervouet A (1985). Evolution tectono-sédementaite de l'avant fosse rifaine du Maroc oriental au Miocène (Tectonosedimentary evolution of the moroccan Rif fore-deep during Miocene). Bulltin de l'institut scientifique Rabat. 9:81-89.

Jalali M (2006). Salinization of groundwater in arid and semi arid zones: An example from Tajarak, western Iran. Environ. Geol. 52:1133-1149.

Kaiser HF (1958). The varimax criteria for analytical rotation in factor analysis. Psychometrika. 23:187-200.

Mahlknecht J, Steinich B, Navaroo de Leon (2004). Groundwater chemistry and mass transfers in the Independence aquifer, central Mexico, by using multivariate statistics and mass-balance models. Environ. Geol. 45:781-795.

Manno E, Vassallo M, Varrica D, Dongarrà G, Hauser S (2007). Hydrogeochemistry and water balance in the coastal wetland area of Biviere di Gela, Sicily, Italy. Water Air Soil Pollut. 178:179-193.

Melish H, Seibt A, Spengenberg E (2008). Long term petrophysical invistegation on geothermal reservoir rocks at simulated *in situ*

conditions. Transp Porous Med. 77:59-78.
Melloul A, Boughriba M, Boufaida M, Snoussi M, Basri M, Toto T, Sadik ML, Jgouni A (2007). Gestion des aquifères côtières par le bias d'une multitude d'approches. Cas de l'aquifère côtier de Saidia (Multitude approaches for coastal aquifers managment: Cas of Saidia coastal aquifer). Hidrogeología y Aguas Subterráneas, IGME, 23:665-675.
Parkhurst DL, Appelo CAJ (1999). User 'guide to PHREEQC (version 2) a computer program for speciaton, reaction path, 1D-transport, and inverse geochemical calculations. US. Geol. Surv. Water Resour., Investig. 99:4259, online version.
Pilla G, Sacchi E, Zuppi G, Brega G, Ciancetti G (2006). Hydrochemistry and isotope geochemistry as tools for groundwater hydrodynamic investigation in multilayer aquifers: A case study from Lomellina, Po plain, South-Western Lombardy, Italy. Hydrogeol. J. 14:795-808.
Petalas CP, Diamantis IB (1999). Origin and distribution of saline groundwaters in the upper Miocene aquifer system, coastal Rhodop area, northestern Greece. Hydrogeol. J. 7:305-316.
Roveri M, Bertini A, Cosentino D, Di Stefano A, Gennari R, Gliozzi E, Grossi F, Iaccarino SM, Lugli, S, Manzi V, Taviani M (2008). A high resolution stratigraphic framwork for the latest Messinian events in the Mediterranean area. Stratigraphy 5:323-342.
Soria JM, Caracuel JE, Corbi H, Dinarès-Turell J, Lancis C, Tent-Manclùs JE, Visearas C, Yébenes A (2008). The Messinian-early Pliocene stratigraphic record in the southern Bajo Segura basin (Betic Cordillera, Spain): Implications for The Mediterranian Salinity crisis. Sediment. Geol. 203:267-288.
Tellam JH, Lloyd JW (1986). Problems in the recognition of seawater intrusion by chemical means: An example of apparent equivalence. Q. J. Eng. Geol. 19:389–398.
Zeryouhi I (1971). Rapport sur l'execution de deux forages de reconnaissances et d'essais dans la plaine du Moyen Kert (Report on the execution of recognition drilling and testing in the Central Middle Kert), Rapp. Inéd. MTPC/DH/DRE, Rabat, p. 5.
Zielhofer C, Faust D, Linstadter J (2008). Late Pleistocene and Holocene alluvial archives in the Southwestern Mediterranean: Changes in fluvial dynamics and past human response. Quaternary Int. 181:39-54.